4.2.2 Target Hall Baffle

4.2.2.1 Baffle Functions and Requirements

The baffle must:

- Prevent mis-steered primary proton beam from causing damage to the horn neck and target cooling/support components.

- Be capable of operating continuously with 3% beam scraping at design luminosity.

- Withstand full intensity of beam for a number of pulses it will take to detect mis-steering of beam and shut beam off.

- Incorporate monitoring that will shut beam off in case of continued large loss of beam on baffle. It may be useful for efficient running that loss of one pulse on baffle not turn off the beam.

- Construction and alignment tolerance of hole through baffle must be 0.5 mm or better.

In addition:

- Incorporate monitoring that allows detection and monitoring of beam-baffle scraping at order of 1% accuracy. (E.g. if 2% of the beam is being scraped, measure (2+/-1)%). Since actual full power beam running is expected be around $2x10^{13}$ during the first couple years running, this means an accuracy of $+/-2x10^{11}$ or better.

- Incorporate monitoring that allows a crosscheck of alignment via e.g. low intensity beam-scan to 0.5 mm.

- Have the baffle move along the beamline with the target, as this increases the available target travel (the overall length for extraction of a broken target/baffle module is limited, and by having the target stick out one end of the carrier at one extreme of motion and the baffle stick out of the carrier at the other extreme one makes maximum usage of this length).

4.2.2.2 Baffle hardware design

The baffle, **Figure 4.2-4**, is mounted with the target to eliminate the expense of another module to support and align it. The baffle and target can be pre-aligned to each other before attachment to the module, and move as a unit. The baffle construction tolerance is 0.2 mm RMS; the goal for overall baffle position accuracy is 0.5 mm, including thermal effects, survey tolerance, and carrier wobble.

.

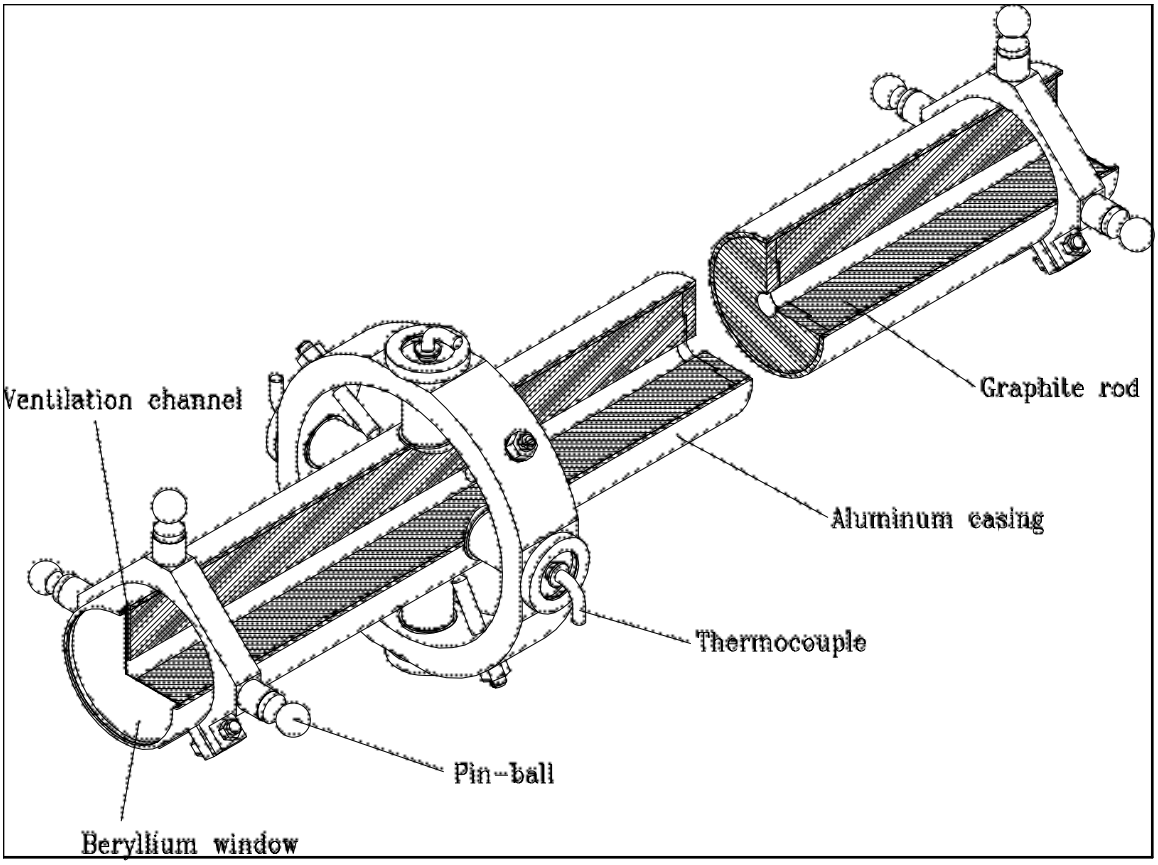

Figure 4.2-4 Baffle. 150 cm long, 11 mm diameter hole, 57 mm diameter graphite core, 61 mm diameter aluminum casing. Cooling fins not shown. Thermocouples will be located near the downstream end of the baffle

Baffle hole size, baffle location – beam accident geometry

The baffle hole is made as large as possible, while still providing protection to the horn and target. **Figure 4.2-5** and **Figure 4.2-6** show the layout of the baffle relative to the target and horn.

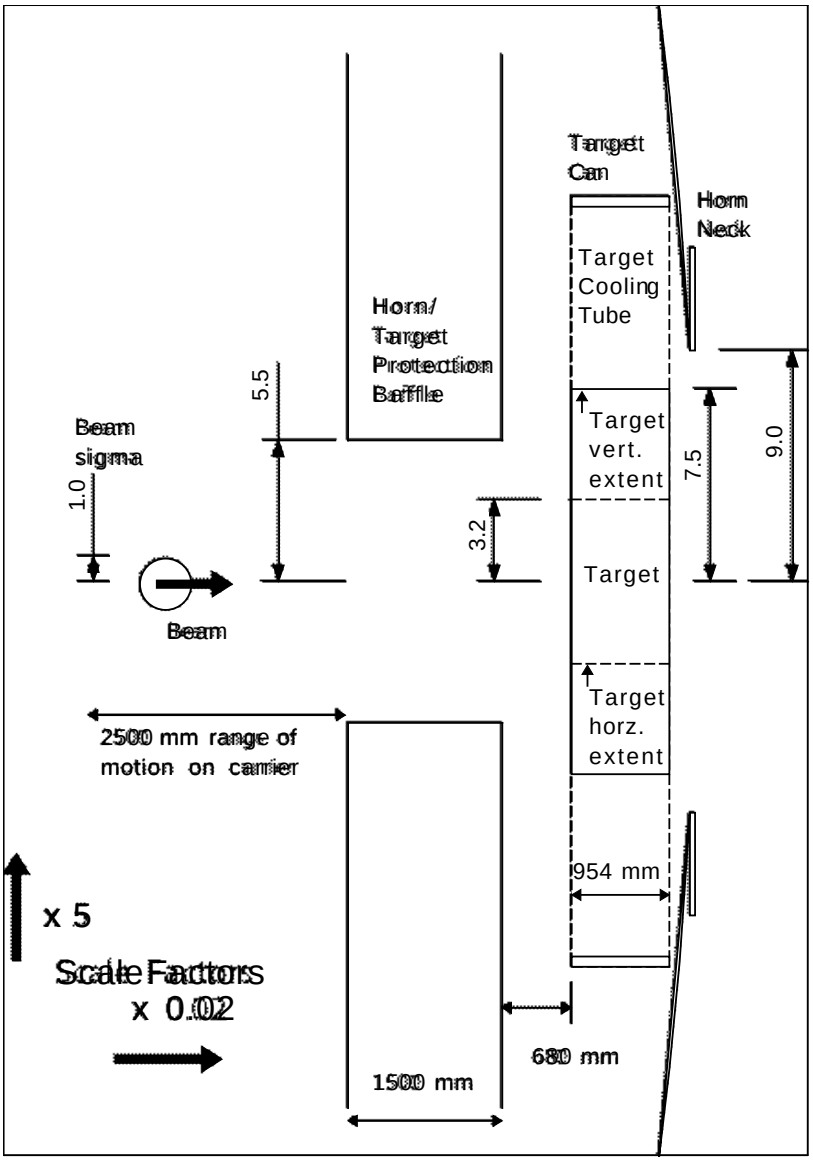

Figure 4.2-5 Plan view of baffle, target, and horn geometry. Since target is rectangular rather than cylindrical, limits of its horizontal and vertical extent are shown. Note large factor between horizontal and vertical scales

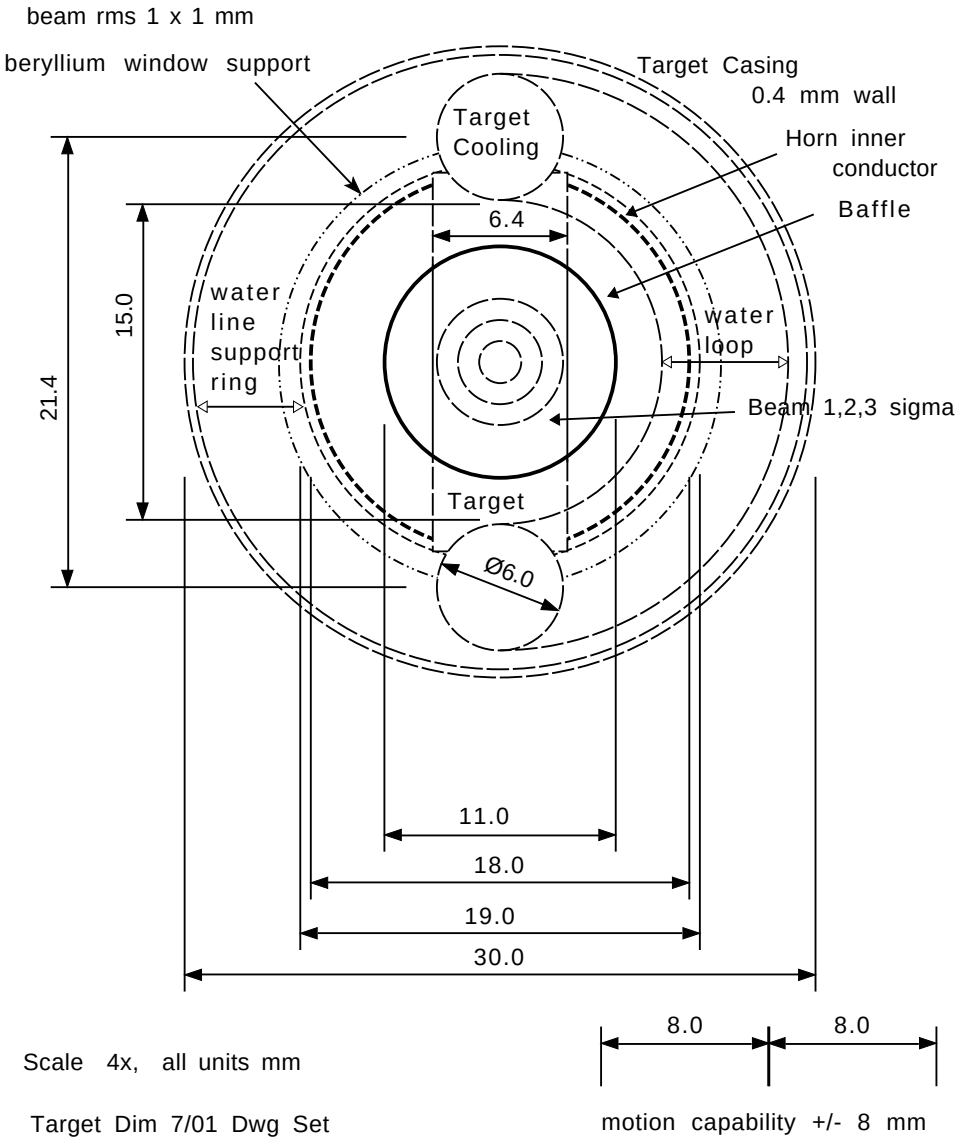

Figure 4.2-6 Beam-eye view of baffle inner radius and comparison to beam spot, target fin, horn neck, and target cooling and support structure.

The horn protection system actually consists of two baffle locations, a relatively large opening after the last bend string (but unfortunately before the last quad), and a second baffle in the target hall. Peter Lucas produced a spreadsheet that takes into account the magnetic field, and gives the maximum radius that the beam could reach while still passing through the two baffles. These limits are set entirely by the two baffles and the intervening magnet, and do not try to identify magnet failures that could actually produce these deviations. Examining some variations run by Adam Para, the pattern is roughly that the fully protected region is the baffle radius plus (0.5 mr horizontal, 0.7 mr vertical) times the distance downstream of the baffle.

Table 4.2-2 lists three items to be protected by the baffle. In it, are derived maximum baffle radii using the above rule of thumb for two cases: (1) having the baffle close to the target, and moving with the target, or (2) at a fixed upstream location which would still allow target movement to the HE location without moving the baffle. Baffle radius is reduced by 0.5 mm to allow for alignment tolerance. Numbers are in coordinate system where horn 1 starts at Z=0cm (i.e. the GNUMI Monte Carlo coordinate system). The horn neck is at (Z,R) = (0.8m,9mm); the top edge is shadowed by the target, so only the horizontal edge is included in the calculation. The target cooling line solder starts at (Z,R) = (-0.35m,7.5mm) at top and bottom of graphite fin; after some distance down target, the graphite contributes to shielding the tube. The cooling loop tube between supply and return is at the end of the target (Z,R) = (0.6m,7.7mm), and is exposed in the horizontal direction.

Baffle hole R(max)	Baffle Z=-2m	Baffle Z=-5m
Horn 1 neck, X direction	7.1 mm	5.6 mm
Target cooling tube, Y direction, LE position	5.8 mm	3.7 mm
Target cooling loop, X direction, LE position	5.9 mm	4.4 mm

Table 4.2-2 Maximum baffle hole radius allowed for different layouts of baffle, horn and target.

From the above table, it is seen that a 5.5 mm radius baffle hole protects the horn for all baffle locations, for all different energy beams. If the target and baffle move together, then a 5.5 mm radius baffle will also protect the target for all beam configurations; however a fixed location baffle would require a smaller hole to protect the target. It is also seen that the X and Y requirements are very similar, and a circular hole thus makes sense. From the above

arguments, the baffle is mounted near the target, moves with the target, and the radius of the hole is selected to be 5.5 mm.

In the current layout, the baffle ends at -103 cm in the Monte Carlo coordinate system, or 68 cm before the leading edge of the target vertical fin.

Baffle material

Calculations have been done of energy deposition, heat rise, and stress for the standard NuMI beam (4e13 protons in a 0.7 mm sigma-x 1.4 mm sigma-y beam spot) hitting Nickel, Copper, Aluminum, and Graphite. Nickel and Copper are clearly unsuitable. Aluminum is marginal; it would exceed its yield point and creep modestly with accident pulses [ref. i]. Graphite is satisfactory [ref. ii]. Beryllium would also work, but is rejected because it would generate mixed waste unnecessarily. We have selected Graphite; it is reasonable to use the same grade selected for the target, ZXF-5Q, since we already have experience with it in the target beam test.

Baffle outer radius

IHEP has proposed shrink-wrapping the graphite in a long aluminum tube [ref. ii]. This provides good thermal contact with the graphite that will be maintained under beam heating in spite of the larger thermal expansion coefficient of aluminum. Also it can be done with high accuracy. The technology they describe would limit baffle diameter to 60 mm; 60 mm would appear to be a reasonable match to NuMI requirements. The graphite diameter is 57.1 mm, which is a standard stock graphite rod size.

Baffle length

Calculations have been done to find out how long the graphite baffle must be to protect the horn inner conductor, the target cooling tube and solder joint to the graphite, and the target ceramic. The position of the baffle was also varied. The position/length selected is that which has the upstream end of the baffle as close to the target as will still provide a good safety margin. This allows the greatest possible target motion. The result chosen is150 cm long baffle with 68 cm spacing between baffle and target fin. Curiously, extending the baffle length in the space between target and baffle further actually makes the energy deposition in the target fixturing worse, although it reduces the energy deposition in the horn neck. Please

see [ref. ii] for derivations of acceptable temperature rises. **Figure 4.2-7** and **Figure 4.2-8** include temperature rises for baffle lengths and positions calculated after [ref. ii] was written. The chosen operating point as shown in **Figure 4.2-8** corresponds to (a) cooling pipe steel stress of 50 MPa compared to 340 MPa yield, (b) Aluminum horn neck stress of 70 MPa compared to 210 MPa yield, (c) ceramic insulator stress of 30 MPa compared to 170 MPa yield, and (d) target solder joint temperature rise of 70 K over approximately 30 deg C operating temperature compared to 340 deg C melting point.

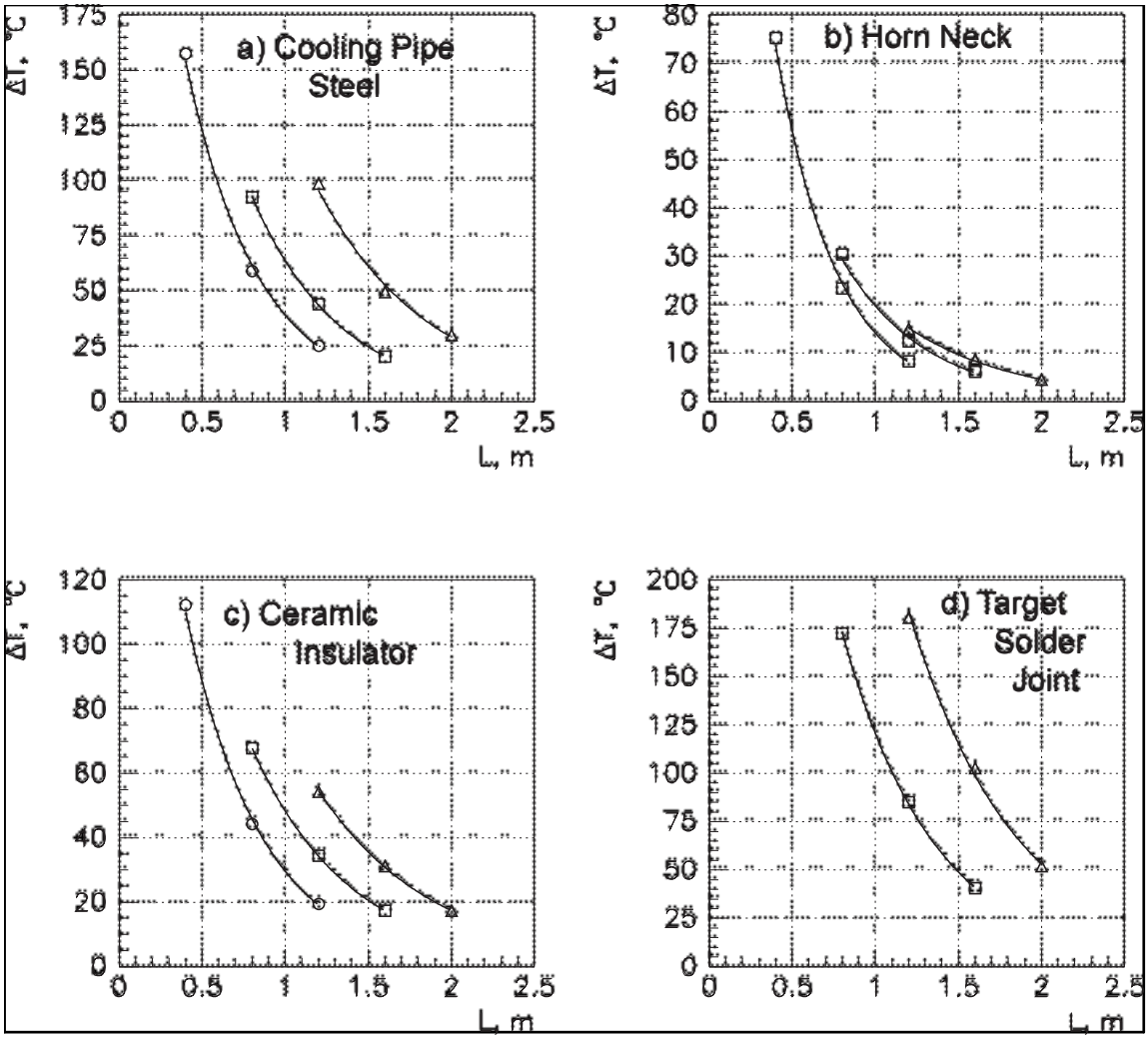

Figure 4.2-7 Temperature rise of protected components for an accident spill as a function of the length of the baffle. The distance Lbt between the downstream end of the baffle and the target vertical fin is 176 cm (circles), 86 cm (boxes), and 41 cm (triangles).

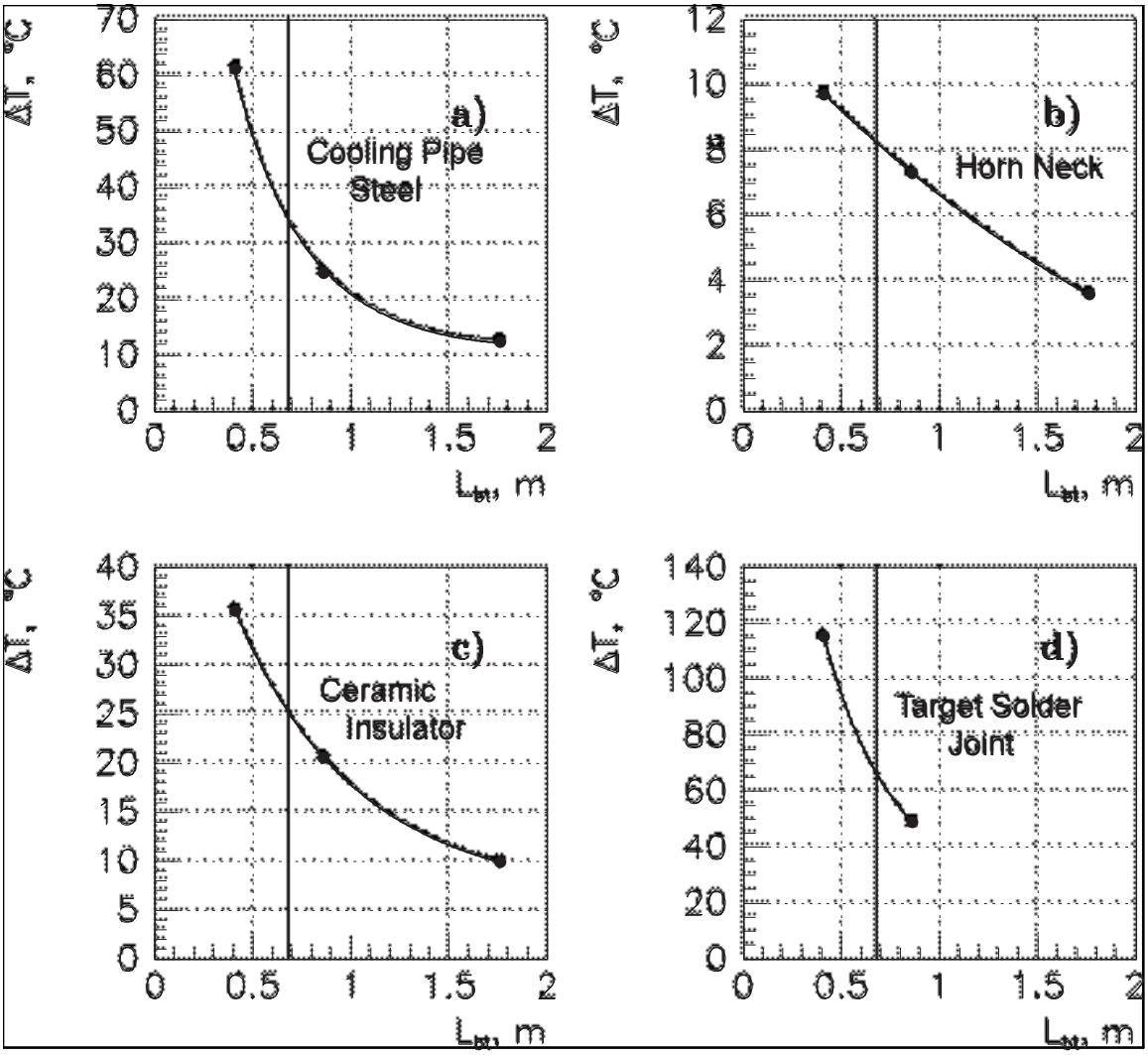

Figure 4.2-8 Temperature rise of protected components for an accident spill as a function of the position of a 1.5 m long baffle. Lbt is the distance from the end of the baffle to the start of the target vertical fin. The chosen design value of 68 cm is marked.

Baffle atmosphere and windows

[ref. ii] documents that the maximum temperature in the core of an accident shower along the inner edge of the baffle is 344 deg C, at which temperature no detectable oxidation is expected. The oxidation threshold (temperature resulting in 1% weight loss in 24 hours) for ZXF-5Q is 450 deg C. Hence an inert atmosphere in the baffle is not required.

Beryllium windows are provided to prevent erosion of the graphite by the strong wind in the target pile. A ventilation hole is provided to prevent air pressure buildup. To help keep ventilation hole clear of debris, the hole should not be oriented upward; to help prevent

contamination falling out of the hole, it should not be oriented down; hence we plan to orient the hole horizontally.

Baffle thermal warp

A thermal gradient laterally across the baffle can be caused by azimuthally asymmetric beam loss, air flow, or cooling fin contact. This would cause the baffle to warp. The following arguments indicate such effects are not a problem for us.

A zeroth order model with a linear temperature gradient across the cylinder gives a warp of the center relative to the ends of ($\alpha TL^2/8w$) where α is the coefficient of thermal expansion, T is the maximum temperature difference, L is the length of the baffle, and w is the width of the baffle. For a warp of 0.5 mm, this implies a temperature difference of 13.3 K for graphite across the baffle. Numerically modeling non-realistic extreme cases where the entire fin cooling was on one half of the baffle or the entire heat deposition was on one half of the baffle for 3% continuous scraping gave only a few degree temperature differences even at the higher temperature downstream end of the baffle. Hence this effect can be safely ignored.

4.2.2.3 Baffle cooling and monitoring

Calorimetric methods are a simple and direct way of monitoring the beam loss on the baffle. For this to work, the cooling of the baffle should be adjusted so that temperature rises are easily measured with standard thermocouples but the baffle will not overheat. The simplest is to rely on heat transfer to the existing air flow, with the addition of fins to increase the heat transfer. However, heat transfer efficiency is hard to precisely calculate a priori, so a large safety factor should be built in for the operating parameters.

Figure 4.2-9 shows the energy distribution when beam hits the front of the baffle [ref. iii]. This corresponds to an average temperature rise of 11 K per pulse at the downstream end of the baffle for full power beam. Since the largest temperature rise is downstream, the monitoring thermocouples should be mounted near the downstream end.

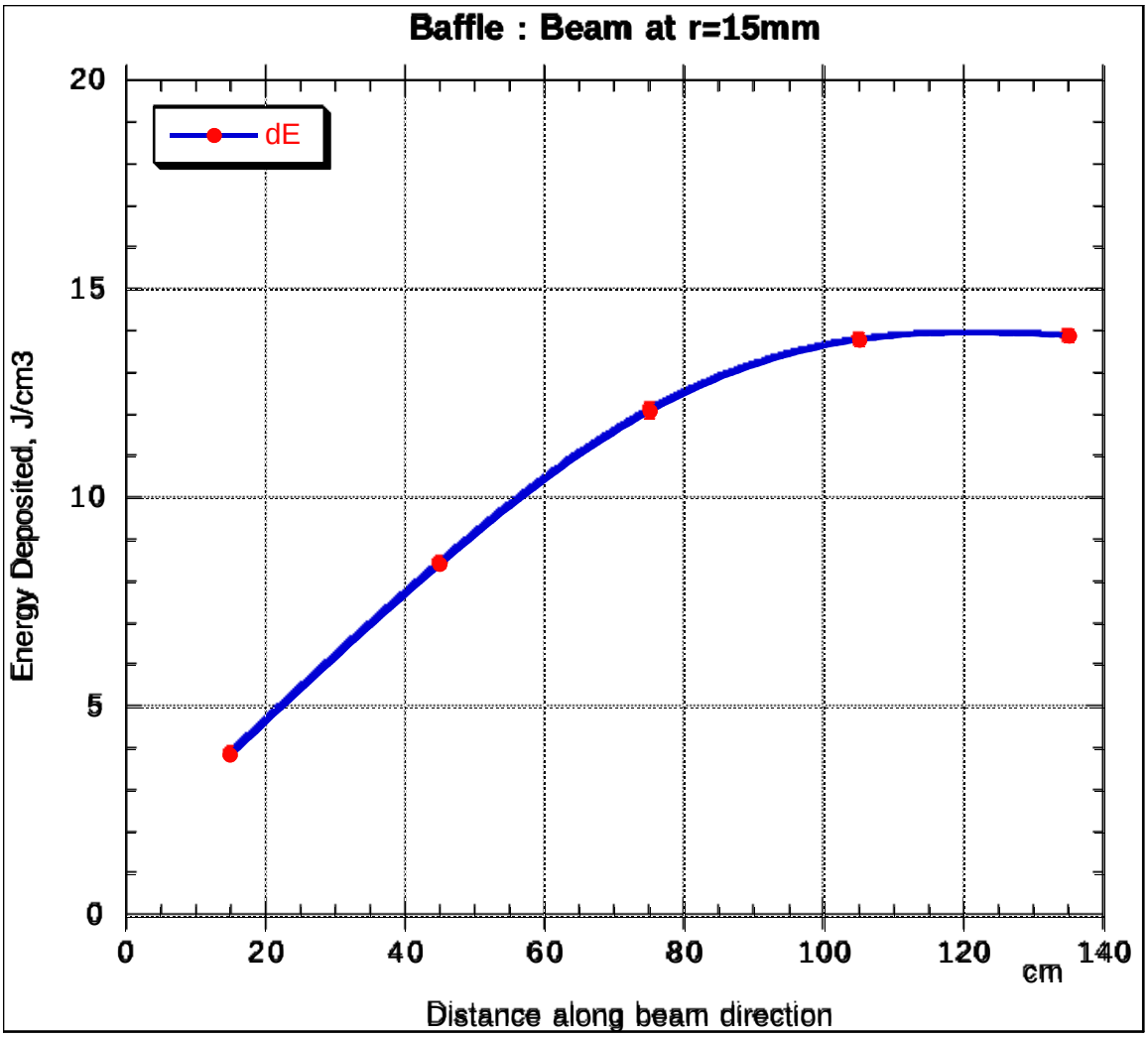

Figure 4.2-9 Energy deposited in baffle (J/cm3/pulse) as a function of position along baffle for 4e13 protons hitting baffle, averaged over 3 cm baffle radius and 30 cm long baffle segments. Integral is 42 kJ/pulse, corresponding to 22 kW at 1.87 second repetition rate, or 5.5% of the 400 kW total beam power.

To first order, the time constant for heat transfer to the cooling air is (Vdc/Ah), and the asymptotic temperature rise is (PV/Ah), where V is the volume of graphite, d is the density of graphite 1.8 g/cm3, c is the specific heat capacity of graphite 0.7 J/gK, A is the surface area of the graphite segment, h is the heat transfer coefficient from baffle to air, and P is the power deposited per unit volume. For a 3 cm radius cylinder, V/A = 1.5 cm. The cooling air flow along the surface of the baffle is about 4 m/s, which would give h~12W/m2K for flow parallel to a fin-less cylindrical baffle [ref. ii]. The actual flow pattern is hard to predict, and with transverse flow the heat transfer coefficient could be double this. For use in selecting a strategy, a hypothetical fin with five times the heat transfer of the cylinder is chosen as a reasonable operating point, and shown in comparison in the table. The cooling air

temperature will be about 16 deg C. Note that [ref. ii] includes full three-dimensional modeling of the heat transfers, with results that agree well at the downstream end of the baffle with the simple approximation given here.

The baffle fin design has not been finalized, but Figure 4.2-10 shows a concept. It consists of two half rings 1.5 mm thick with pins 2 mm in diameter. Pins of 15 mm height are located with period 7 mm along the circumference and 9 mm along the baffle. The internal radius of a half ring is the same as the external radius of the baffle casing. These half rings are pressed to the baffle casing via a stainless steel clamp, providing pressure about 10-20 MPa. Such a pressure should provide a good thermal contact between radiator and casing. Another

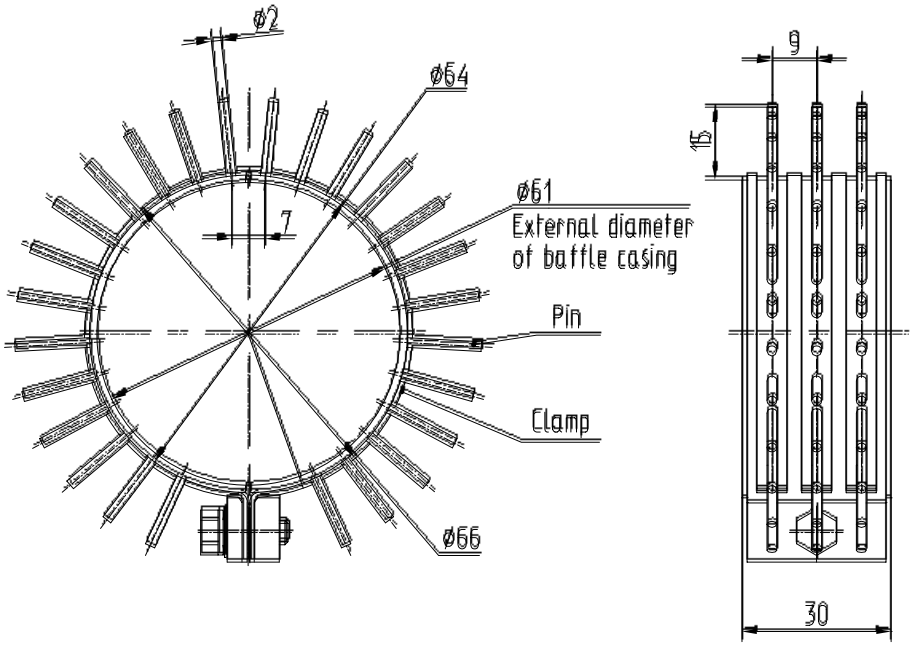

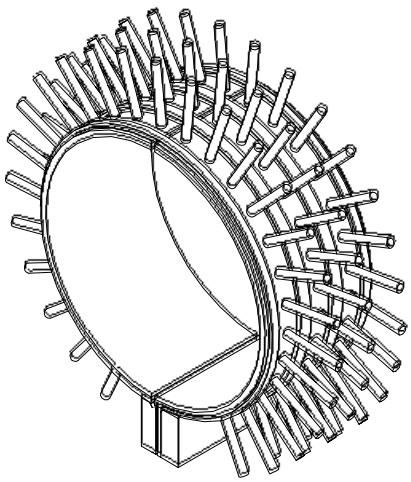

Accident scenario

To prevent damage to the aluminum baffle tube, an interlock will be set to prevent further beam pulses at a thermocouple readback of about 120 deg C. The interlock could be set lower if found to be operationally desirable. This would prevent more than at most a dozen continuous accident pulses; however the interlock will probably not be set tight enough to trip the beam from a single accident pulse. With the fin, the baffle will cool off in a few minutes, allowing one to turn the beam back on quickly.

Continuous scraping

We are optimistic that beam scraping will be low. The fin design nevertheless would allow 3% continuous beam scraping with a safety factor of 2 in the heat transfer coefficient h before reaching the 120 deg C trip point.

The 19 K temperature rise per 1% beam loss is an order of magnitude larger than needed for monitoring the beam loss at the required level, providing a large safety factor on the value of h being larger than the design specification.

Backgrounds to the calorimetric monitoring of the baffle scraping have also been calculated. The energy deposit in the baffle is 0.10 J/cm3/pulse for 1% scraping, compared to 0.04 J/cm3/pulse from interactions in the target pile air and 0.0002 J/cm3/pulse backscatter from the target [ref. iii].

Note that the thermal monitoring does not give pulse-by-pulse monitoring of the scraping, but an average with a few minute time constant. We have not yet found an argument showing a necessity for pulse-by-pulse monitoring of scraping.

Calibration

The actual temperature response of the baffle will be calibrated during commissioning by steering 100% of the beam at low intensity on to the baffle. Note that a constant beam intensity should be maintained for a period of several time constants for this measurement.

Commissioning alignment scan

The fin parameter set also allows an alignment check of the baffle via beam scan during commissioning, or whenever one wants to recheck alignment. It is conservative to turn down beam power during scans; beam intensity as low as $8x10^{11}$ protons per pulse is easy to achieve. Such a single pulse (2% of maximum beam) into the baffle would produce only a 0.2 K temperature rise in the baffle, so one would need to use a large number of pulses per point (say 30 over a one minute period), or else a higher intensity beam (in which case one could limit the repetition rate) to produce a robust thermocouple response. With the standard 1 mm RMS beam spot, an alignment check accuracy of a fraction of 1 mm would be expected, based on experience with similar temperature scans done during the NuMI target test.

Usable signals from the alignment check baffle scan will most likely also be detected in the horn 1 alignment ionization chamber and the hadron monitor in front of the absorber, providing redundancy.

Since the baffle and target are pre-aligned on a common carrier, the combination of baffle scan and Budal-monitor target scan can demonstrate that the combined baffle/target system is at the correct angle as well as in the correct position.

4.2.2.4 Effect of scraping on the neutrino spectrum

The effect on the neutrino spectrum of beam tails hitting the baffle has been modeled in GNUMI, and is illustrated in **Figure 4.2-11**. The effect of scraping is mostly significant between 5 GeV and 8 GeV. In a 10-ktyear exposure, there will be of order 500 events in this range collected in the MINOS far detector, giving a statistical error of 4%. Thus knowing a scraping correction to 1% accuracy would keep the systematic error negligible compared to the statistical error. As shown in the figure, 1% beam scraping produces about a 1% change in the double ratio (beam scraping correction), hence measuring the scraping to +/- 1% of the total beam power is a reasonable specification.

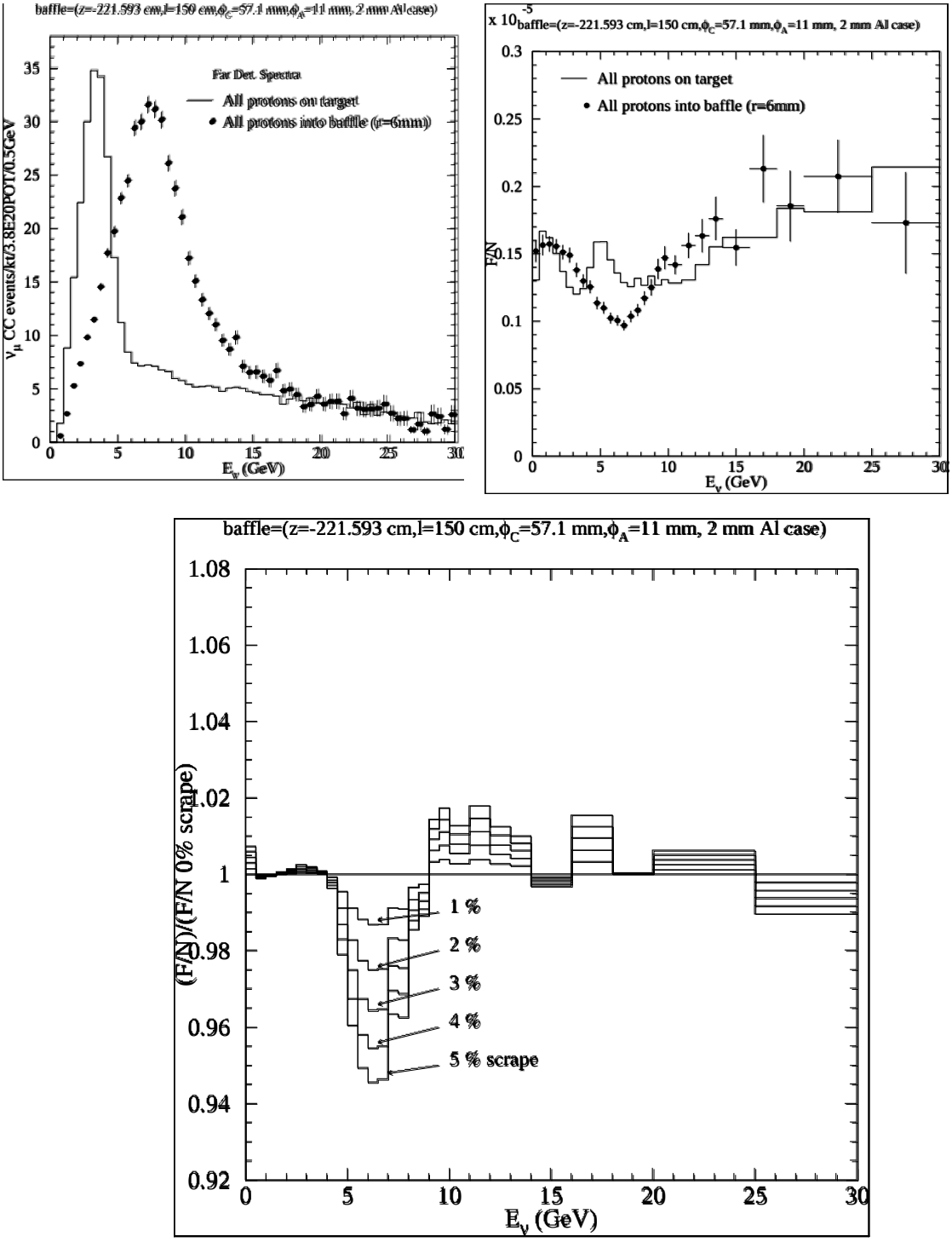

Figure 4.2-11 Effect of various amounts of beam-baffle scraping on neutrino spectrum. Top plots show spectra separately for 100% of beam on target or baffle. (Mark Messier, 6/12/02)

It would be nice to keep the scraping to less than 1%, so that no correction at all would need to be applied. For a gaussian beam with 1 mm RMS, 99% of the beam is within 3 mm radius. In our case, the baffle hole is 5.5 mm radius, and even after allowing for 0.5 mm alignment tolerances the loss from a gaussian beam would be negligible. However, only experience with the real beam will tell us if there are significant non-gaussian tails, or jitter in the beam position that cause losses on the baffle.

Note this simulation had baffle to target distance of 37 cm instead of our current choice of 68 cm, but that should have only a minor effect. In a similar study with the baffle a couple meters further back, Brajesh Choudhary found the scraping sensitivity to be twice as large, which may be another motivation for keeping the baffle close to the target.

References

---

[i] Thermal Stress Analysis of Numi Baffle – II, MSG-EAR-0282, Bob Wands, 4/2/01 and Thermal Stress Analysis of NuMI Baffle, MSG-EAR-00279, Bob Wands, 11/8/00.

[ii] Technical Design of the Target Pile Protection Baffle-draft, S.Filippov, V. Garkusha, R. Gibadullin, F. Novoskoltsev, I. Ponimash, T. Ryabova, V. Zarucheisky, (IHEP) 4/30/02.

[iii] MARS Simulation: Baffle Heating, B. Lundberg, 6/9/02.